A triple suicide gene strategy that improves therapeutic effects and incorporates multi-modality molecular imaging for monitoring gene-functions

Ligang Xing[1,2], **Xiaorong Sun**[2,3], **Xuelong Deng**[2], **Khushali Kotedia**[4], **Pat B. Zanzonico**[4], **Ellen Ackerstaff**[4], **Jason A. Koutcher**[4], **C. Clifton Ling**[4], and **Gloria C. Li**[2,4]

[1]Department of Radiation Oncology and Shandong Key Laboratory of Radiation Oncology, Shandong Cancer Hospital and Institute, 440 Jiyan Road, Jinan, Shandong, China 250117

[2]Department of Radiation Oncology, Memorial Sloan-Kettering Cancer Center, 1275 York Avenue, New York, NY, USA 10065

[3]PET-CT center, Shandong Cancer Hospital and Institute, 440 Jiyan Road, Jinan, Shandong, China 250117

[4]Department of Medical Physics, Memorial Sloan-Kettering Cancer Center, 1275 York Avenue, New York, NY, USA 10065

Abstract

Gene-directed enzyme prodrug therapy (GDEPT), or suicide gene therapy, has shown promise in clinical trials. In this preclinical study using stable cell lines and xenograft tumor models, we show that a triple-suicide-gene GDEPT approach produce enhanced therapeutic efficacy over previous methods. Importantly all the three genes (thymidine kinase, cytosine deaminase, and uracil phosphoribosyltransferase) function simultaneously as effectors for GDEPT and markers for multimodality molecular imaging (MMI), using positron-emission-tomography (PET), magnetic resonance-spectroscopy (MRS), and optical (fluorescent and bioluminescent) techniques. It was demonstrated that MMI can evaluate the distribution and function/activity of the triple-suicide-gene. The concomitant expression of these genes significantly enhances prodrug cytotoxicity and radiosensitivity *in vitro* and *in vivo*.

Corresponding author: Gloria C. Li, Ph. D. Departments of Medical Physics and Radiation Oncology, 1275 York Avenue, P.O. Box 72, New York, NY 10021, Tel: 1-646-888-2118, Fax: 1-646-422-0247, lig@mskcc.org.

The authors disclose no potential conflicts of interest.

Introduction

Multimodality molecular imaging (MMI), using positron emission tomography (PET), magnetic resonance spectroscopy, (MRS) and optical (fluorescent and bioluminescent) techniques, offers powerful tools in unraveling biological processes in cancer diagnosis and treatment.[1]. MMI also play a crucial role in developing and optimizing gene therapy for cancer, such as gene-directed enzyme prodrug therapy (GDEPT) or "suicide gene therapy".[2,3] Suicide genes such as herpes simplex virus type-1 thymidine kinase (HSV-1 TK), cytosine deaminase (CD), and uracil phosphoribosyltransferase (UPRT) simultaneously function as effector genes for GDEPT and marker genes for MMI. As an effector, TK converts the prodrug ganciclovir (GCV) into toxic products, and as a marker, leads to the trapping of the marker substrate ^{124}I-FIAU (or ^{18}F-FEAU, ^{18}F-FHBG, etc) for PET imaging.[4–6] Similarly, CD and UPRT function as effector genes, with CD converting the prodrug 5-FC to the chemotherapeutic drug 5-FU, and UPRT converting 5-FU to the cytotoxic compound (fluoro-nucleotides, FNuc). As marker genes they permit MRS imaging (MRSI) of the spatial distributions of 5-FC, 5-FU and FNuc, thus assessing the function and activity of the CD and UPRT genes.[7–9] Individually, MRS and PET are powerful molecular imaging methods each of which has contributed to improve cancer gene therapy. The combined use of both modalities may be even more powerful, motivating the development of combined PET/MRI units.[10,11]

Since GDEPT employing single gene of HSV1-TK, CD, or UPRT has been demonstrated to be effective, efforts were focused on GDEPT combining two of these genes (double suicide gene therapy). Several studies have demonstrated that integrated CD/5-FC and HSV1-TK/GCV strategies is more effective with synergistic effects when compared with either strategy alone.[12,13] Simultaneous expression of CD and UPRT genes could lead to synergistic effects resulting in increased sensitivity to 5-FC.[14,15] Among double suicide gene therapy strategies, the combination of HSV1-TK/GCV and CD/5-FC is most widely studied and has been evaluated in clinical trials[16,17]. Subsequently, a reporter gene system (the human sodium iodide symporter, hNIS) was incorporated into a double suicide gene (TK/CD) adenovirus, and Na^{99m}TcO$_4$ SPECT images demonstrated gene expression after virus injection into human prostate cancer.[18] Thus, it was suggested that MMI can be used to monitor adenovirus-mediated suicide gene therapy.[18]

The aim of the present preclinical study is to demonstrate that the therapeutic efficacy of the triple-suicide-gene approach is improved relative to previous methods, and that multimodality molecular imaging can be used to monitor the delivery, and evaluate the distribution and function/activity of the triple-suicide-gene.

Material and Methods

Plasmids

Three plasmids were constructed: 1) pCMV-TK/eGFP contains the *HSV1-tk* and *egfp* fusion gene under the control of a cytomegalovirus (CMV) promoter and a neomycin resistant gene, 2) pCMV-CD/mDsRed containing the *cd* (of *Saccharomyces cervisiae*) and monomeric dsred (*mDsRed*) fusion gene and 3) pCMV-CD/UPRT/mDsRed containing the

cd, *uprt* (of *Haemophilus influenzae*) and *mDsRed* fusion gene under the control of the CMV promoter. The latter two plasmids contain the hygromycin B resistance gene.[7]

Cell Cultures and Stably Transfected Cell Lines

R3327-AT rat prostate carcinoma cells were maintained in Dulbecco's Modified Eagle medium (DMEM; Mediatech, Herndon, VA) supplemented with 10% fetal bovine serum, 100 U/ml penicillin and 100 μg/ml streptomycin (Gemini, West Sacramento, CA). The cells were co-transfected with two plasmids, pCMV-CD/mDsRed and pCMV-TK/eGFP, or pCMV-CD/UPRT/mDsRed and pCMV-TK/eGFP using Lipofectamine2000 (Invitrogen, Carlsbad, VA) according to the manufacturer's instructions. Subsequently, the transfected cells were cultured in medium containing Hygromycin B (0.2 mg/ml; Roche, Mannheim, Germany) and G418 (0.5 mg/ml, Calbiochem, San Diego, CA). Stable transfectants were selected with fluorescence activated cell sorting (FACS) using a cell sorter (MoFlo™, Dako, Carpinteria, CA). Single-cell-derived clones with the positive mDsRed and eGFP expression were isolated, expanded, their mDsRed and eGFP expression verified by flow cytometry, and used for further experiments. All cells were grown as monolayers at 37°C in a humidified incubator with 5% CO_2 and 95% air. Stably transfected cells were designated as TKCD cells and TKCDUPRT cells, respectively (eGFP and mDsRed were omitted for simplicity)

Western Blot Analysis

The sheep anti-yCD polyclonal antibody was purchased from Biotrend (Cologne, Germany) and the anti-HSV1-TK monoclonal antibody was kindly provided by Dr. W.C. Summers (Yale University, New Haven, CT). The secondary antibodies were the horseradish peroxidase-labeled bovine anti-sheep IgG (Santa Cruz, Santa Cruz, CA) or sheep anti-mouse IgG (Pierce, Rockford, IL), respectively. The protein expression was visualized using the Supersignal chemiluminescent substrate (Pierce).

Flow Cytometric Analysis

The expression of eGFP and mDsRed was analyzed by flow cytometry using the cell sorter (MoFlo™, Beckman Coulter). Parental cells, cells constitutively expressing only TK/eGFP or CD/mDsRed were analyzed in parallel as negative control, eGFP-positive or mDsRed-positive controls, respectively.

Fluorescence Microscopy

The cells were fixed with freshly prepared 4% paraformaldehyde for 10 minutes and rinsed twice with PBS. The fluorescent images were acquired at 575 nm wavelength for mDsRed and at 488 nm for eGFP using a fluorescence microscope (Axiovert 200M, Carl Zeiss MicroImaging GmbH_Göttingen, Germany).

Drug Cytotoxicity, radiation survival, and Colony Formation Assay

Cells were treated with GCV (Sigma-Aldrich, St. Louis, MO), 5-FC (InvivoGen, San Diego, CA) or 5-FU (InvivoGen) at various concentrations for 24 hr. Thereafter cells were trypsinized, counted, serially diluted, and plated into 60 mm dishes. After incubation for 10–

14 days, colonies were stained with crystal violet and counted. Cell survival curves were constructed by plotting the surviving fractions as a function of drug concentration. For radiosensitization experiments, cells were treated with GCV or 5-FC alone or in combination for 24 hr, and then irradiated with graded doses using a Cs-137 unit (Mark 1 model 68, Shephard and Associate, San Fernando CA) at ~2.0Gy/min. The cell survivals were determined by colony-formation assay and plotted as a function of radiation doses.

Animal Xenograft

Animal protocols were approved by the Institutional Animal Care and Use Committee at MSKCC. Tumor xenografts were formed by injecting 3×10^6 cells subcutaneously into the hind legs of 6–8 week old nude mice (athymic nu/nu; NCI Frederick Cancer Research Institute, Frederick, MD). Each tumor was measured with digital caliper in three orthogonal dimensions (a, b and c), and tumor volume was calculated as πabc/6. Experiments were performed when the tumors reached a volume of ~ 500 mm^3 for imaging study, or a volume of ~150 mm^3 for tumor growth delay study.

^{19}F MR Spectroscopy and MRS Imaging

In vivo ^{19}F MRS was performed using a Bruker 7T spectrometer.[9] Mice were anesthetized with isoflurane and positioned in a specially designed animal holder. ^{19}F MR spectra were acquired and averaged over 10 min before and after the *i.v.* administration of 150mg/kg 5-FU or 5-FC for a maximum of 1 hr using a single pulse with a TR of 1s and sweep width of 15 kHz. A glass sphere (18μl) filled with 75 mmol/L sodium fluoride (NaF) was used as an external reference for quantitation. The MR time domain data were analyzed using XsOs NMR (Columbia University). The spectral area of the acquired data was obtained from a Lorentzian fit to the spectra after line broadening (30Hz). Metabolite ratios were calculated by normalizing their resonance-peak areas to that of NaF. Graphic representation of the spectroscopic data (5-FC/NaF, 5-FU/NaF and FNuc/NaF) shows the average ± SD of the given ratio at each time point.

Preceding the acquisition of ^{19}F-MRSI, T$_2$-weighted proton images were acquired for anatomic localization of the MRSI spectra. Imaging parameters included: FOV= 30mm × 30mm, matrix size= 256 × 256, 6 averages, TR= 2s and TE= 30ms. The MRSI sequence was used to acquire slice-selective two-dimensional images in the coronal plane with respect to the tumor at 7 T with 13-phase encode steps at effective in-plane resolutions of 3.75 mm × 3.75 mm with a FOV= 30mm × 30mm, matrix size= 8 × 8, slice thickness = 4mm, 1024 data points with a spectral width of 15 kHz, 60° flip angle, and TR = 1s and 4092 scans.

^{124}I-FIAU microPET imaging

Two to three hours after MRS measurements, 7.4 MBq of ^{124}I-FIAU was *i.v.* injected with the thyroid blocked by adding SSKI (Super Saturated Potassium Iodide) to their drinking water 1 day ahead. The whole-body microPET images were acquired 16 -18 hr afterwards at the Focus 120 microPET scanner (Concorde Microsystems; Knoxville, TN) under anesthesia. In general, a minimum of ~10 million events were acquired in 20–40 min, depending on the administered activity and the time post injection. The image data were corrected for non-uniformity of response, dead time count losses, and physical decay. An

empirically determined system calibration factor was used to convert voxel count rates (adjusted for the [124]I branching ratio) to activity concentrations, and the resulting data were normalized to the administered activity to yield percent of the injected dose per gram of tissue (%ID/g).

In vivo/ex vivo Fluorescent Imaging

Immediately after PET imaging, whole-body fluorescent images were acquired with a Maestro™ imaging system (CRi, Woburn, MA) under anesthesia. The fluorescent images of eGFP and mDsRed were acquired using the 455 nm (435–480nm) excitation/490 nm long-pass emission filters and the 523 nm (503–548nm) excitation/560nm long-pass emission filters, respectively. The images were unmixed with the tissue autofluorescence spectrum using linear least-squares optimization. After *in vivo* imaging, the tumors were dissected and their fluorescent images were acquired. Immediately after the *ex vivo* imaging, the tumors were embedded in O.C.T, frozen with dry ice, and cut into 8-μm sections for autoradiography and fluorescent microscopy.

Autoradiography and Fluorescent Microscopy of Tumor Sections

To acquire the distributions of [124]I-FIAU in the tumor sections, phosphor plate imaging was employed with 13 hours exposure. Digital autoradiographs were processed using a Fujifilm BAS-1800II bioimaging analyzer (Fuji Photo Film Co. Japan). Whole tumor eGFP and mDsRed fluorescent images from the same sections were acquired using a fluorescent microscope (Axiovert 200M) after the autoradiography exposure as previously described.[19]

Tumor Growth Delay

The mice bearing TKCD or TKCDUPRT tumors were divided into five groups and treated with: (1) PBS, (2) 500 mg/kg 5-FC plus 30 mg/kg GCV, *i.p.*a (standard dose), (3) 25 mg/kg 5-FC plus 1.5 mg/kg GCV *i.p.* (low dose), (4) radiation (3Gy), or (5) radiation combined with drug treatments (25 mg/kg 5-FC plus 1.5 mg/kg GCV *i.p.,* 2h before radiation). The tumors were irradiated using the Cs-137 unit (Mark 1 model 68) within a home-made animal holder. The treatments were applied once a day for 5 days. Ten mice were used in each group. For six mice, the tumor volume was measured three times a week until the average volume reached ~1500 mm^3. The tumor volume relative to those at the beginning of treatments was calculated and plotted as a function of time after treatments. The difference in time (days) of tumor volume reaching ~1500 mm^3 for treated groups relative to controlled group (relative growth delay) was calculated and compared. For other four mice, the tumors were dissected at 24 hr after the last treatment, fixed with 4% paraformaldehyde, embedded with paraffin and cut into 4 μm sections for the immunohistochemistry staining.

Immunohistochemistry Staining and Imaging Acquisition

The detection of proliferation and apoptosis in tumor sections was achieved by immunohistochemical staining using the rabbit anti-Ki-67 and anti-cleaved caspase-3 primary antibodies and goat anti-rabbit second antibodies, respectively (Cell Signaling Technology, Danvers, MA). Finally the sections were stained with hematoxylin-eosin. The sections were scanned on a digital histology platform (Mirax, Carl Zeiss) at x200

magnification. Composite images of sections were generated from individual microscopic images by the software Mirax viewer. Ki-67 and CCP3 staining positive cells were counted and compared between different groups.

Statistical analysis

Averages are presented as the mean±SE. Difference in cytotoxicity and radiosensitivity was determined using the Student's t test. The difference in Ki-67 or CCP3 staining was analyzed using the t test, and tumor growth delay using 1-way ANOVA. A *P* value of <0.01 was considered statistically significant.

Results

In Vitro characterization of cells expressing gene-multiplex

We established rat prostate cancer cell lines which stably express both TK/eGFP and CD/mDsRed (designated as TKCD cells), or both TK/eGFP and D/UPRT/mDsRed (designated as TKCDUPRT cells), respectively. Expression of the transduced fusion genes were assessed by Western blot, flow cytometry and fluorescent microscopy. Immunoblot with HSV1-TK antibody showed a 65-kDa band in the TKCD and the TKCDUPRT samples, and in the TK control sample (cells only expressing TKeGFP)(Fig. 1A, left panel). As shown in the right panel of Fig. 1A, analysis with anti-CD antibody revealed a 43-kDa band in the TKCD cell sample and the CD control (cells only expressing CDmDsRed), and a 66-kDa band in the TKCDUPRT cell sample and the CDUPRTmDsRed control (cells only expressing CDUPRTmDsRed). These bands corresponded to the predicted molecular weights of the various fusion proteins, respectively. As further validation, fluorescence activated cell sorting (FACS) analysis showed that 96% of TKCD cells (Fig. 1B, upper panel) and 98% of TKCDUPRT cells (Fig. 1B, lower panel) are positive for both eGFP and mDsRed. Fluorescence microscopy of TKCD and TKCDUPRT cells exhibit strong eGFP and mDsRed signals (Fig. 1C).

The expression of TK and CD in the TKCD and TKCDUPRT cells enhanced the cellular sensitivity to GCV and 5-FC, compared to that of the parental cells. Similarly, the expression of UPRT in the TKCDUPRT cells enhanced their sensitivity to 5-FU and 5-FC, relative to that of the TKCD cells (Fig. 1D). These observations evince the function and activity of the HSV1-TK, CD and UPRT enzymes in the transduced cells.

Multi-modality and multi-parametric molecular imaging

When transplanted into nude mice, the TKCDUPRT cells form tumors which allow multi-modality and multi-parametric imaging studies of transgene expression/function, all in the same tumor as illustrated in the schematics of Fig. 2A.

As CD catalyzed the conversion of 5-FC to 5-FU, and UPRT facilitated that of 5-FU to 5-FUMP, ^{19}F MRS was used to assess the expression/function of CD and UPRT in transplanted tumors. The upper panel of Figure 2b displays ^{19}F MR spectra acquired at various times after a bolus injection of 150 mg/kg 5-FC. Whereas the 5-FC signal was persistent, its conversion to 5-FU was visible at 10 min, followed by the accumulation of

FNuc at later times. The left lower panel of Fig. 2B showed discernable accumulation of FNuc at 10–20 min, and steady increase afterwards. Parental R3327-AT tumors did not metabolize 5-FC, and 5-FU and FNuc were not detected (data not shown). To provide spatial information of metabolic data, ^{19}F NMR chemical shift images were acquired at different locations in the tumor. These results are displayed as a matrix of FNuc spectra, overlaid on a T2-weighted proton image of the tumor (right lower panel, Fig. 2B). This data demonstrated reasonable uniformity of CDUPRT expression/function in the tumor.

Similar data were acquired in mice with TKCDUPRT tumors injected with 5-FU. As shown in left and middle panel in Supplementary Figure 1A, the MRS data showed a steady decrease of 5-FU, concomitant with the accumulation of FNuc, beginning with the first measurement time point of ~ 10 min after injection. The 2D "matrix" showed reasonably uniform distribution of FNuc overlaid on a T2-weighted proton image (right panel, Supplementary Figure 1A).

After the NMR studies, the same TKCDUPRT tumors were assessed for their constitutive expression of TK *in vivo*. The microPET images clearly showed significant uptake of ^{124}I-FIAU in the TKCDUPRT tumors, evincing the expression of TK (Fig. 2C, and Supplementary Fig. 1B). Uptake in some normal tissues (bladder, thyroid, and bowel) is also noted. For further corroboration, *ex vivo* nuclear imaging (autoradiography) was performed on tumor sections using a phosphor plate. The resulting images quantified the distribution of ^{124}I-FIAU radioactivity in the tumor sections with high spatial resolution of ~ 50μm (Fig. 2E and Supplementary Fig. 1D).

Both eGFP and mDsRed expression were detected in the tumors in live mice (*in vivo*), or in excised tumors (*ex vivo*), as shown in Fig. 2D and Supplementary Fig. 1C, respectively. Fluorescent microscopic images (Fig. 2F and Supplementary Fig. 1E) acquired for the same tumor section as in the autoradiograph (Fig. 2E and Supplementary Fig. 1D) showed similar overall distributions of eGFP, mDsRed and ^{124}I-FIAU.

The expression of TK, CD and UPRT on cell and tumor response to 5-FC, GCV and radiation

In vitro, the simultaneous expression of these genes significantly enhances the cytotoxicity to GCV and 5-FC. Whereas TKCDUPRT cells were sensitive to GCV and 5-FC administered as single agent (Fig. 1D), concurrent treatment with both GCV and 5-FC resulted in much greater cytotoxicity (Fig. 3A, left panel) with significant synergistic action between the two prodrugs (Supplementary Figure 2). TKCD cells were also sensitive to combined treatment of GCV and 5-FC (Fig. 3A, right panel), but ~20-fold higher 5-FC doses were needed to induce the similar levels of cytotoxicity.

To study the by-stander effect, admixtures of parental and transfected cells, in the ratio of 4:1, were treated with GCV and 5-FC alone, or in combination. The results (Supplementary Fig. 3A and 3B) indicated that the admixture of parental and TKCDUPRT cells was much more sensitive than that of parental and TKCD cells for all treatment scenarios.

To provide *in vivo* validation of the efficacy of triple suicide gene approach, tumor-bearing mice were treated with the standard doses of GCV (30 mg/kg) and 5-FC (500 mg/kg), or lower doses (1.5 mg/kg GCV, and 25 mg/kg 5-FC), daily for 5 days. The volumes of TKCDUPRT tumors, measured at various times, showed significant growth delay at the lower drug dose (left panel, Fig. 3B, triangles), and complete tumor regression at the standard dose, with no recurrence within the 40 day observation period (left panel, Fig. 3B, solid squares). Growth delay was also observed in TKCD tumors treated with GCV and 5-FC (Fig. 3B, right panel), but the effect was much less relative to that of TKCDUPRT tumors.

At the histological level, in TKCDUPRT tumors treated with the standard dose, cell proliferation was significantly attenuated (Fig. 4A, upper panel) and extensive apoptosis was observed (Fig. 4B, upper panel). In quantitative analysis the Ki-67 positive counts in 5-FC +GCV treated and controlled tumors was 90.7 ± 7.2 and 328.9 ± 12.8 (Fig. 4A, right panel, $P<0.01$); and the CCP3 positive index in treated and controlled tumors was 152.3 ± 15.5 and 26.1 ± 3.1 (Fig. 4B, right panel, $P<0.01$). In treated TKCD tumors, while cellular proliferation was decreased (Fig. 4B, lower panel), the Ki-67 positive index in 5-FC+GCV treated and control tumors was 122.3 ± 7.7 and 210.9 ± 14.8 (Fig. 4A, right panel, $P<0.01$). Also, the apoptotic index were slightly increased (Fig. 4A, lower panel, with CCP3 positive index in 5-FC+GCV treated and controlled tumors of 37.3 ± 3.5 and 16.9 ± 1.5 (Fig. 4B, right panel, $P>0.01$).

As was previously shown, expression TK, CD and UPRT led to enhanced response to produrg treatment. Here we present data showing that cells and tumors expressing TK, CD and UPRT and treated with prodrugs are more radiosensitive. As shown in Figure 5A, TKCD and TKCDUPRT cells have similar radiosensitivity without prodrug. Single agent treatment with GCV or 5-FC slightly enhanced the radiation response, but combined treatment with both 5-FC and GCV resulted into greater radiosensitization. In addition, the degree of radiosensitization is much higher in TKCDUPRT cells than TKCD cells, such that the 5-FC dose needed is only 1/50 to achieve the same radiosensitivity. A similar effect was observed for cell mixture of 80% parental and 20% TKCDUPRT cells (Supplementary Fig. 2C). In growth delay assay, radiation (3Gy/fraction per day for 5 days) alone slightly delayed the tumor growth, but when combined with low dose treatment of GCV and 5-FC, produced significant tumor growth delay (Fig. 5B). Again, the effect was greater in TKCDUPRT tumors. The relative growth delay (days) due to 5-FC+GCV and 5-FC+GCV +radiation treatments was much longer in TKCDUPRT tumors than that in TKCD tumors ($P<0.01$).

Discussion

In previous efforts, we constructed expressing vectors of CDUPRT fused with red fluorescent protein (mDsRed), and HSV1-TK fused with green fluorescent protein (eGFP), and generated tumor models in which expression of the respective gene-complexes can be monitored with MRS/optical, or PET/optical imaging, respectively.[7,19] In the present study, we report for the first time the triple-suicide-gene approach, using TK, CD, and UPRT. Importantly, all three genes function simultaneously as effectors for GDEPT and markers for

MMI. It is demonstrated that MMI can evaluate the distribution and function/activity of the triple-suicide-gene. The concomitant expression of these genes significantly enhances prodrug cytotoxicity and radiosensitivity *in vitro* and *in vivo*. Our data convincingly demonstrate in proof-of-principle that integrating MMI and triple-suicide-gene therapy can significantly improve the efficacy of combinative cancer treatment.

Both PET and MRI techniques are important in developing and optimizing gene therapy, initially in laboratory setting, and then translated into clinical studies. Jacobs et al. [20] employed [124]I-FIAU PET to monitor liposomal vector-mediated HSV1-TK gene expression in five patients with recurrent glioblastomas. Their preliminary findings showed that FIAU-PET-imaging of HSV-1-*tk* expression in patients is feasible and that vector-mediated gene expression may predict the therapeutic effect. Quantitative MRSI of 5-FU pharmacokinetics in patients has been reported previously.[21] Clinical trials of TK-CD cancer gene therapy [16] suggest that MRSI and PET monitoring of gene therapy with MRSI and PET could have immediate implications for the investigation of gene therapy strategies. Our data clearly showed that the prodrug activation in TKCDUPRT-expressing tumor could be measured with [124]I FIAU microPET (for TK) and ^{19}F MRSI (for CDUPRT). As hybrid PET/MRI scanner has being developed from the preclinical prototype to clinical platforms [22], visualization and quantification of triple suicide gene expression/function in a single system will become available.

There has been steady progress in applying gene-directed enzyme prodrug therapy (GEDPT), or suicide gene therapy, to cancer treatment, from single suicide gene therapy (e.g. using HSV1-TK with GCV, or CD with 5-FC) to the combined use of two suicide genes (e.g. CD and HSV1-TK, or CD and UPRT), resulting in improved tumoricidal effect for different tumors.[12–15,23] Both the *in vitro* and *in vivo* data in the present study (Fig. 3–5 and supplementary Fig. 2) clearly demonstrated that the triple suicide gene therapy approach is more effective in eradicating tumors than double suicide gene therapy employing HSV1-TK/GCV and CD/5-FC, which has been tested in clinical trials [16,17].

The potential advantage of suicide gene therapy relevant for clinical application is its radiosensitization effect, as demonstrated in our study. We clearly showed that the co-expression of HSV1-TK, CD and UPRT triple genes, not only significantly increased the sensitivity of GCV and 5-FC, but also improved the radiosensitizing effect of GCV and 5-FC, relative to that induced by double suicide gene HSV1-TK and CD strategy (Fig. 5). In this regard, it has been shown that HSV-1 TK/GCV gene therapy may inhibit the repair of radiation-induced sublethal DNA damage.[24] Others have suggested that the radiosensitization in CD/5-FC and CD/UPRT/5-FC approaches is mediated through the inhibition of thymidylate synthase by 5-FdUMP, resulting in the depletion of deoxythymidine monophosphate pools and increased DNA strand break, as well as redistribution of cells to the radiosensitive early S phase.[25] Previously, we have demonstrated that CDUPRT/5-FC approach has greater radiosensitization effect than the CD/5-FC system.[15] Therefore, it is not surprising that significant tumor control effects were found as triple suicide gene approach combined with radiation.

The difficulty in achieving efficient gene delivery to all cells in a tumor mass *in vivo* is a major limitation for successful cancer gene therapy. Therefore, the bystander effect is an important feature of suicide gene therapy, whereby the surrounding but untransduced cells are inactivated by the diffusion of toxic metabolites derived from the transduced cells.[26] Our data clearly demonstrated that a strong bystander effect was associated with the triple suicide gene approach. Mixed, heterogeneous cell populations in which only 20% of cells expressing TK, CD and UPRT were much more sensitive to GCV and 5-FC treatments than cells expressing TK and CD (Supplementary Fig. 2A). More importantly, an enhanced radiosensitizing effect was observed in the cell population consisted of only 20% cells expressing TK, CD and UPRT after treatment of GCV plus 5-FC (Supplementary Fig. 2B).

The studies were done in nude mice and eliminated the acquired immune response which has been shown to be active, at least in HSV1-tk therapy. It suggests that our approach might work better in intact animals. Whereas this study involved the use of stably transfected cell lines and associated tumor models with different transgene expression, drug sensitivity and growth rates, future studies are planned to translate this strategy to clinical application. Specifically, we are generating adenovirus vectors armed with TK, CD and UPRT genes to deliver them into *in vivo* tumor models and to test whether triple gene transduction following GCV and 5-FC treatment will improve the efficacy of radiotherapy. As shown in present study, molecular imaging using PET and MRI can be used to monitor the function/activity of a triple suicide gene. While the clinical utility of molecular imaging in suicide gene therapy must await clinical trials, we can illustrate its potential use with the following example. Suppose in a particular patient, PET and/or MRSI imaging suggest heterogeneity in the expressions of the TK or CD/UPRT genes in the tumor, one might consider additional injection of viral vectors to target that portion of the tumor with weak suicide gene expression. Clinical studies will be needed to evaluate this approach in cancer patients.

Supplementary Material

Refer to Web version on PubMed Central for supplementary material.

Acknowledgments

References

1. Frangioni JV. New technologies for human cancer imaging. J Clin Oncol. 2008; 26:4012–4021. [PubMed: 18711192]

2. Rome C, Couillaud F, Moonen CT. Gene expression and gene therapy imaging. Eur Radiol. 2007; 17:305–319. [PubMed: 16967261]

3. Bhaumik S. Advances in imaging gene-directed enzyme prodrug therapy. Curr Pharm Biotechnol. 2011; 12:497–507. [PubMed: 21342105]

4. Yaghoubi SS, Barrio JR, Namavari M, Satyamurthy N, Phelps ME, Herschman HR, et al. Imaging progress of herpes simplex virus type 1 thymidine kinase suicide gene therapy in living subjects with positron emission tomography. Cancer Gene Ther. 2005; 12:329–339. [PubMed: 15592447]

5. Gambhir SS, Barrio JR, Phelps ME, Iyer M, Namavari M, Satyamurthy N, et al. Imaging adenoviral-directed reporter gene expression in living animals with positron emission tomography. Proc Natl Acad Sci U S A. 1999; 96:2333–2338. [PubMed: 10051642]

6. Tjuvajev JG, Finn R, Watanabe K, Joshi R, Oku T, Kennedy J, et al. Noninvasive imaging of herpes virus thymidine kinase gene transfer and expression: a potential method for monitoring clinical gene therapy. Cancer Res. 1996; 56:4087–4095. [PubMed: 8797571]

7. Xing L, Deng X, Kotedia K, Ackerstaff E, Ponomarev V, Clifton Ling C, et al. Non-invasive molecular and functional imaging of cytosine deaminase and uracil phosphoribosyltransferase fused with red fluorescence protein. Acta Oncol. 2008; 47:1211–1220. [PubMed: 18661431]

8. Hamstra DA, Lee KC, Tychewicz JM, Schepkin VD, Moffat BA, Chen M, et al. The use of 19F spectroscopy and diffusion-weighted MRI to evaluate differences in gene-dependent enzyme prodrug therapies. Mol Ther. 2004; 10:916–928. [PubMed: 15509509]

9. Gade TP, Koutcher JA, Spees WM, Beattie BJ, Ponomarev V, Doubrovin M, et al. Imaging transgene activity in vivo. Cancer Res. 2008; 68:2878–2884. [PubMed: 18413756]

10. Judenhofer MS, Wehrl HF, Newport DF, Catana C, Siegel SB, Becker M, et al. Simultaneous PET-MRI: a new approach for functional and morphological imaging. Nat Med. 2008; 14:459–465. [PubMed: 18376410]

11. Catana C, Wu Y, Judenhofer MS, Qi J, Pichler BJ, Cherry SR. Simultaneous acquisition of multislice PET and MR images: initial results with a MR-compatible PET scanner. J Nucl Med. 2006; 47:1968–1976. [PubMed: 17138739]

12. Aghi M, Kramm CM, Chou TC, Breakefield XO, Chiocca EA. Synergistic anticancer effects of ganciclovir/thymidine kinase and 5-fluorocytosine/cytosine deaminase gene therapies. J Natl Cancer Inst. 1998; 90:370–380. [PubMed: 9498487]

13. Boucher PD, Im MM, Freytag SO, Shewach DS. A novel mechanism of synergistic cytotoxicity with 5-fluorocytosine and ganciclovir in double suicide gene therapy. Cancer Res. 2006; 66:3230–3237. [PubMed: 16540675]

14. Erbs P, Regulier E, Kintz J, Leroy P, Poitevin Y, Exinger F, et al. In vivo cancer gene therapy by adenovirus-mediated transfer of a bifunctional yeast cytosine deaminase/uracil phosphoribosyltransferase fusion gene. Cancer Res. 2000; 60:3813–3822. [PubMed: 10919655]

15. Xing L, Sun X, Deng X, Kotedia K, Urano M, Koutcher JA, et al. Expression of the bifunctional suicide gene CDUPRT increases radiosensitization and bystander effect of 5-FC in prostate cancer cells. Radiother Oncol. 2009; 92:345–352. [PubMed: 19433338]

16. Freytag SO, Movsas B, Aref I, Stricker H, Peabody J, Pegg J, et al. Phase I trial of replication-competent adenovirus-mediated suicide gene therapy combined with IMRT for prostate cancer. Mol Ther. 2007; 15:1016–1023. [PubMed: 17375076]

17. Freytag SO, Stricker H, Pegg J, Paielli D, Pradhan DG, Peabody J, et al. Phase I study of replication-competent adenovirus-mediated double-suicide gene therapy in combination with conventional-dose three-dimensional conformal radiation therapy for the treatment of newly diagnosed, intermediate- to high-risk prostate cancer. Cancer Res. 2003; 63:7497–7506. [PubMed: 14612551]

18. Barton KN, Stricker H, Brown SL, Elshaikh M, Aref I, Lu M, et al. Phase I study of noninvasive imaging of adenovirus-mediated gene expression in the human prostate. Mol Ther. 2008; 16:1761–1769. [PubMed: 18714306]

19. He F, Deng X, Wen B, Liu Y, Sun X, Xing L, et al. Noninvasive molecular imaging of hypoxia in human xenografts: comparing hypoxia-induced gene expression with endogenous and exogenous hypoxia markers. Cancer Res. 2008; 68:8597–8606. [PubMed: 18922936]

20. Jacobs A, Voges J, Reszka R, Lercher M, Gossmann A, Kracht L, et al. Positron-emission tomography of vector-mediated gene expression in gene therapy for gliomas. Lancet. 2001; 358:727–729. [PubMed: 11551583]

21. Li CW, Negendank WG, Padavic-Shaller KA, O'Dwyer PJ, Murphy-Boesch J, Brown TR. Quantitation of 5-fluorouracil catabolism in human liver in vivo by three-dimensional localized 19F magnetic resonance spectroscopy. Clin Cancer Res. 1996; 2:339–345. [PubMed: 9816177]

22. Boss A, Bisdas S, Kolb A, Hofmann M, Ernemann U, Claussen CD, et al. Hybrid PET/MRI of intracranial masses: initial experiences and comparison to PET/CT. J Nucl Med. 2010; 51:1198–1205. [PubMed: 20660388]

23. Qiu Y, Peng GL, Liu QC, Li FL, Zou XS, He JX. Selective killing of lung cancer cells using carcinoembryonic antigen promoter and double suicide genes, thymidine kinase and cytosine deaminase (pCEA-TK/CD). Cancer Lett. 2012; 316:31–38. [PubMed: 22099873]

24. Freytag SO, Kim JH, Brown SL, Barton K, Lu M, Chung M. Gene therapy strategies to improve the effectiveness of cancer radiotherapy. Expert Opin Biol Ther. 2004; 4:1757–1770. [PubMed: 15500404]

25. Hwang HS, Davis TW, Houghton JA, Kinsella TJ. Radiosensitivity of thymidylate synthase-deficient human tumor cells is affected by progression through the G1 restriction point into S-phase: implications for fluoropyrimidine radiosensitization. Cancer Res. 2000; 60:92–100. [PubMed: 10646859]

26. Khatri A, Zhang B, Doherty E, Chapman J, Ow K, Pwint H, et al. Combination of cytosine deaminase with uracil phosphoribosyl transferase leads to local and distant bystander effects against RM1 prostate cancer in mice. J Gene Med. 2006; 8:1086–1096. [PubMed: 16832832]
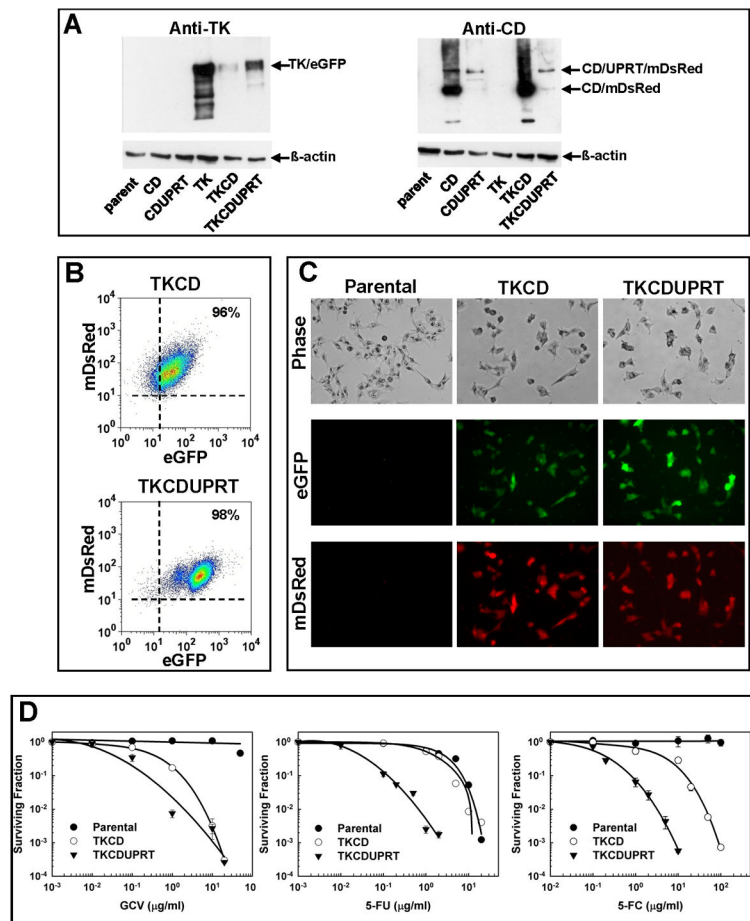
Figure 1. Characteristics of the cell line*s* stably expressing both (i) TK/eGFP and CD/UPRT/ mDsRed (designated as TKCDUPRT cells), and (ii) TK/eGFP and CD/mDsRed (designated as TKCD cells)

(A) Western Blot. Anti-HSV1-TK monoclonal antibody (left panel) and anti-CD polyclonal antibody (right panel) was used, with re-stained β-actin as internal control. Protein samples from parental cells, and the cells expressing CD/mDsRed (designated as CD cells), CD/ UPRT/mDsRed (desingated as CDUPRT cells) or TK/eGFP (designated as TK cells) were used as controls. The protein bands for CD/mDsRed (43 kDa), CD/UPRT/mDsRed (73 kDa) or TK/eGFP (65 kDa) were indicated by arrows on the right side of the western blots respectively.

(B) Flow cytometry analysis of TKCD (top panel) and TKCDUPRT (bottom panel) cells, with eGFP intensity along the x-axis, and mDsRed the y-axis. The gates (dashed lines) were set to include <1% of (i) parental cells, (ii) cells expressing only eGFP, and (iii) cells expressing only mDsRed. The % of cells positive for both eGFP and mDsRed are given in the upper right corner.

(C) Phase-contrasted (upper panel) and fluorescence (eGFP - middle panel, and mDsRed - lower panel) microscopic images at x200 magnification, of parental (left column), TKCD (middle column) and TKCDUPRT cells (right column).

(D) Surviving fractions of parental (●), TKCD (○) and TKCDUPRT (▼) cells, after a 24 hr exposure to different concentrations of GCV (left panel), 5-FU (middle panel) or 5-FC (right panel). Each point represents the mean ± SE from three experiments.
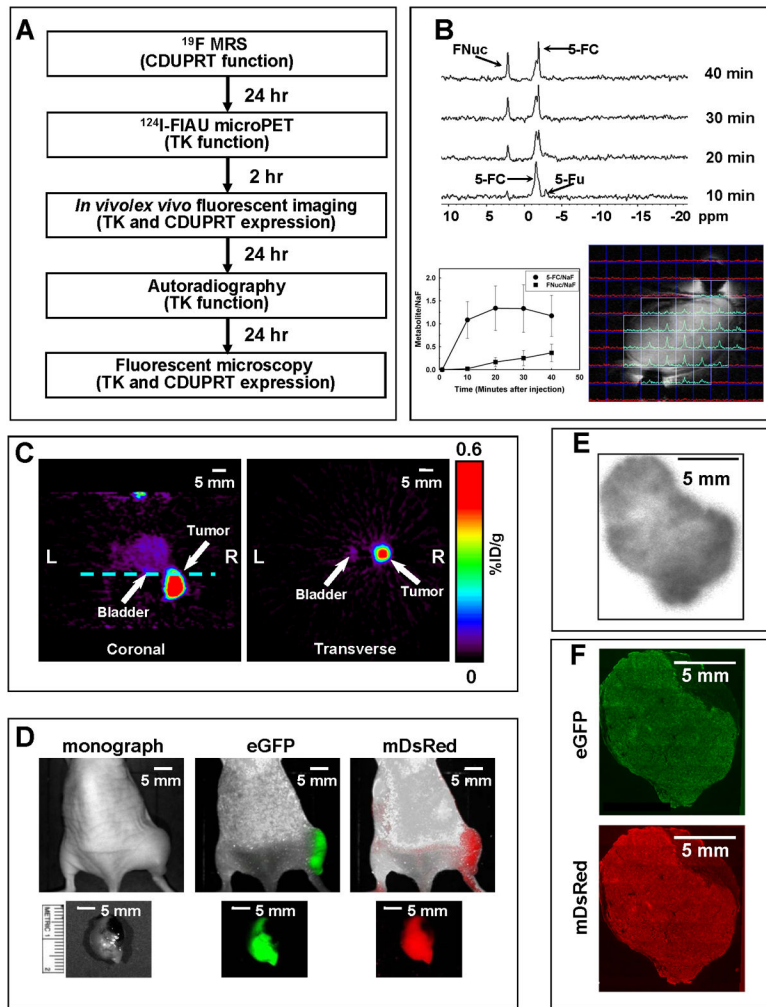
Figure 2. Multimodality imaging of transgene expression/function from the same mouse bearing a TKCDUPRT tumor xenograft

(**A**) A flowchart showing the sequence of multimodality imaging: ^{19}F MRS imaging performed on day 1 (data shown in **B**), [124]I-FIAU PET and *in vivo/ex vivo* optical imaging performed on day 2 (data shown in **C** and **D**, respectively), autoradiography on day 3 (data shown in **E**), and microscopic fluorescence images on day 4 (data shown in **F**).

(**B**) ^{19}F MRS data on CDUPRT function: Upper panel - serial ^{19}F MR spectra of 5-FC, 5-FU and anabolite FNuc, acquired at 10, 20, 30 and 40 min after *i.v.* injection of 150 mg/kg 5-FC; lower left panel - the ratios of 5-FC/NaF (●) and FNuc/NaF (■) (mean ± SE) measured and plotted as function of time; lower right panel - a "map" of the acquired FNuc spectra, displayed as a matrix overlaid on the corresponding [1]H-MR images.

(**C**) MicroPET imaging of TK function at 16–18 hr after *i.v* injection of [124]I-FIAU (7.4 MBq). Coronal (left panel) and transverse (right panel) images are shown. The dashed line in the coronal image indicated the position of the transverse image.

(**D**) The upper panels show *in vivo* monography, eGFP and mDsRed fluorescent images of the same mouse. The lower panels show *ex vivo* images of the same tumor.

(**E–F**) Autoradiograph and microscopy fluorescent images (eGFP -upper panel and mDsRed- lower panel). The images in **F** are from the same section and that in **E** from an adjacent section.
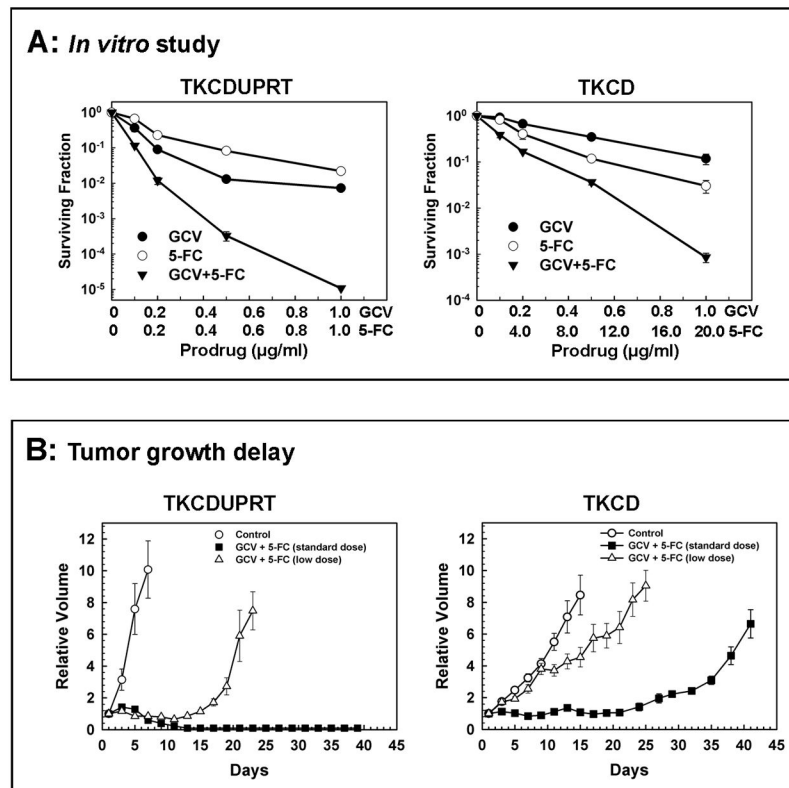
Figure 3. Effect of co-expression of TK, CD and UPRT on cellular and tumor response to GCV and 5-FC

(A) Surviving fractions of TKCDUPRT (left panel) or TKCD (right panel) cells treated with various dose of GCV (●), 5-FC (○), or GCV + 5-FC (▼) for 24 hr.

(B) Tumor growth kinetics in mice bearing TKCDUPRT tumors (left panel) or TKCD tumors (right panel): (○) untreated, (■) treated with 5 daily standard dose of GCV (30 mg/kg) and 5-FC (500 mg/kg), (△) treated with 5 daily lower dose of GCV (1.5 mg/kg) and 5-FC (25 mg/kg). Six mice were used for each group.
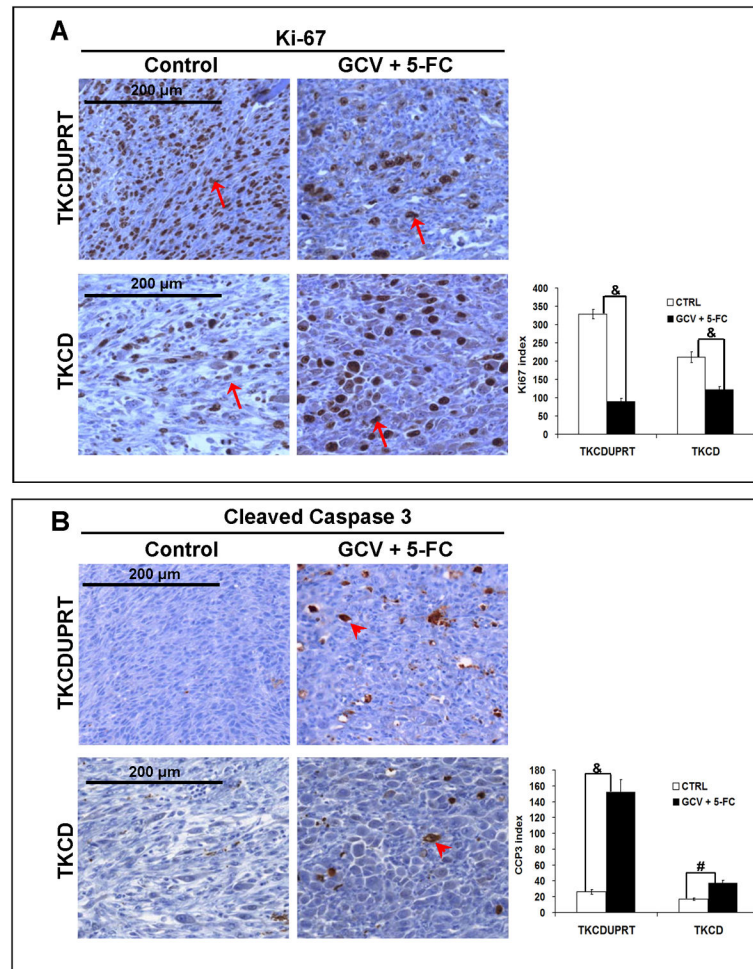
Figure 4. Immunohistochemistry staining of Ki-67 (A) and cleaved Caspase-3 (B)
This was performed in TKCDUPRT-expressing (top panel) and TKCD-expressing (bottom panel) tumors in untreated mice (control) or in mice injected with GCV (30 mg/kg) and 5-FC (500 mg/kg). The number Ki-67 and CCP3 staining positive cell was counted in 200 μm × 200 μm magnified fields at the composited images (10 fields/each tumor) and compared between treated tumors and controlled tumors. &: $P<0.01$, #: $P>0.01$.
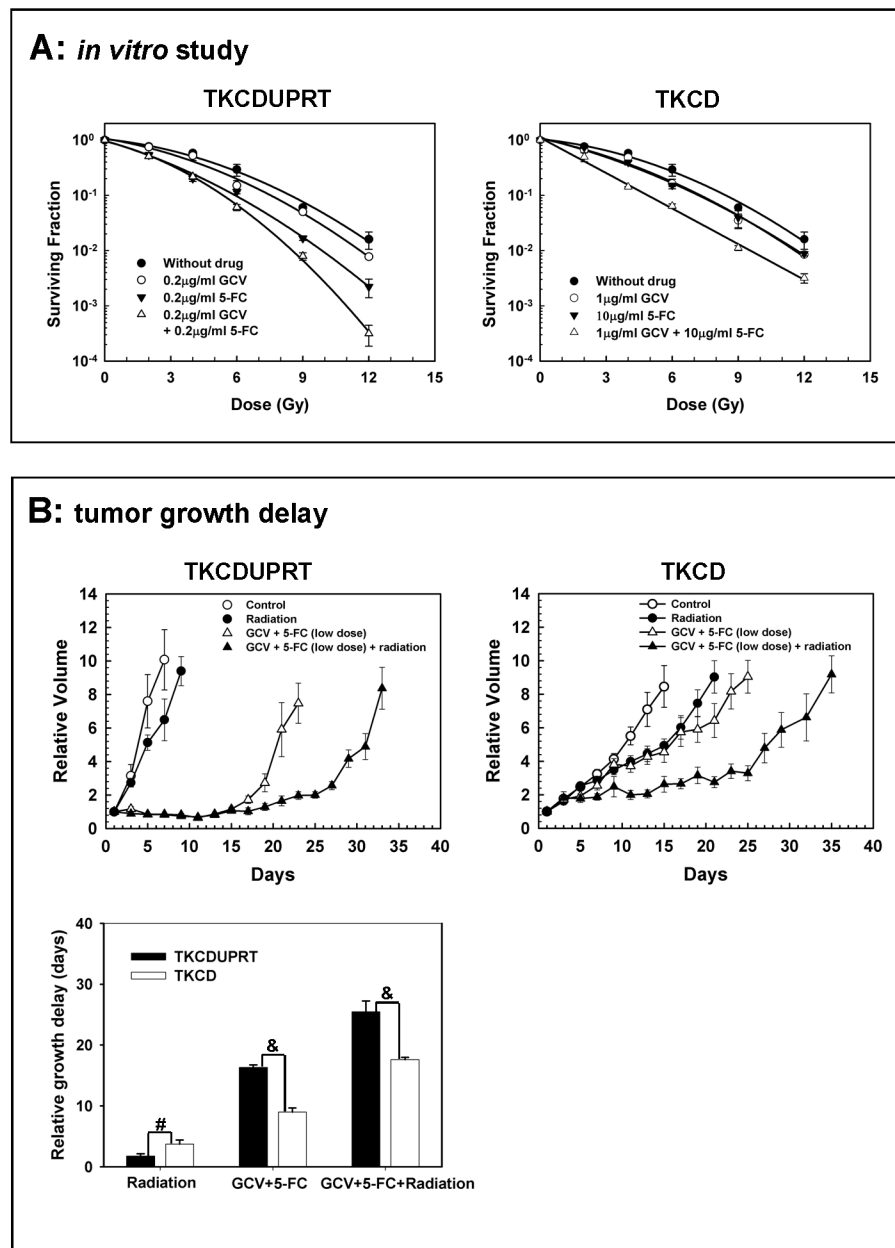
Figure 5. Effect of co-expression of TK, CD and UPRT on cellular and tumor response to graded doses of radiation, by itself, or in combination with GCV and 5-FC

(**A**) Surviving fractions of TKCDUPRT cells (left panel) or TKCD cells (right panel) treated with radiation alone (●), or in combination with GCV (○), 5-FC (▼) or both GCV and 5-FC (△). Mean ± SE were calculated from three experiments.

(**B**) Growth kinetics of TKCDUPRT tumors (left panel) or TKCD tumors (right panel): (○) untreated, (●) radiation only (3Gy/day for 5 days), (△) treated with lower doses of GCV (1.5 mg/kg) and 5-FC (25 mg/kg), (▲) radiation (3Gy/day for 5 days) after lower dose of GCV (1.5 mg/kg) and 5-FC (25 mg/kg). Six mice were used for each group. Time of tumor

volume reaching ~1500 mm^3 relative to the controlled group was compared among groups (1-way ANOVA). Error bars represent the SE of six mice. &: *P*<0.01, #: *P*>0.01.